Morphology and Optical Properties of Fluorene-Based Ladder-type Poly(para-phenylenes): Origin of Low-Energy Emission

ARTICLE *in* THE JOURNAL OF PHYSICAL CHEMISTRY C · APRIL 2009

Impact Factor: 4.77 · DOI: 10.1021/jp8090733

6 AUTHORS, INCLUDING:

Song Qiu
Chinese Academy of Sciences
20 PUBLICATIONS **383** CITATIONS

SEE PROFILE

Huan Wang
Northeast Petroleum University
28 PUBLICATIONS **524** CITATIONS

SEE PROFILE

Yuguang Ma
Chinese Academy of Sciences
310 PUBLICATIONS **6,296** CITATIONS

SEE PROFILE

Morphology and Optical Properties of Fluorene-Based Ladder-type Poly(*para*-phenylenes): Origin of Low-Energy Emission

Linlin Liu, Song Qiu, Baoling Wang, Huan Wang, Zengqi Xie, and Yuguang Ma*

State Key Laboratory for Supramolecular Structure and Materials, Jilin University, 2699 Qianjin Avenue, Changchun 130012, People's Republic of China

Received: October 14, 2008; Revised Manuscript Received: February 8, 2009

The stability of fluorene-based compounds and polymers, especially at the bridged C-9 position, under photoirradiation and thermal treatment has widely claimed attention. The real chromophore group of low-energy emission in fluorene-based compounds and polymers is debatable for fluorenone, and the aggregate is difficult to distinguish. We report the morphology and optical properties of two fluorene-based ladder-type poly(*p*-phenylene)s (LPFs) with the target to explore the real chromophore group of low-energy emission. The basic comparison of LPFs with different substitutions and degraded degree testify the low-energy emission is relating to oxidized products but not packing order. The molecular distance is then adjusted by doping degraded LPF into an inert matrix, which shows that the low-energy emission is as strong as in bulk when the average molecular distance is larger than 1.2 nm. These results suggest fluorenone is the chromophore group of low-energy emission and rule out aggregate, especially fluorenone-based aggregates that require a molecular distance smaller than 0.4 nm.

Introduction

Bridged poly(*p*-phenylene) polymers (PPP) have been extensively studied over the past few decades. In these polymers, the adjacent phenylenes are bridged by a methylene, which is substituted by alkyls to increase the solubility. The most typical materials are polyfluorene (PF) and ladder PPP (LPPP) (Chart 1). High quantum efficiency of fluorescence and blue emission make this class of materials promising candidates for high-efficiency polymer-based electroluminescent (EL) devices.[1] However, the difficulties often encountered are that the blue emitting turns to green for the appearance of a low-energy emission band in the range between 2.0 and 2.5 eV from solution to film and/or during the operation of polymer light emitting diodes (PLEDs). Thus, efforts are focused to find the origin of the green emission and recover the blue emission.[1]

Earlier, the low-energy emission was considered as the emission from molecular aggregation induced by the heat treatment, especially the Joule heat generated during the operation of PLEDs.[2] More recent evidences suggest that the low-energy emission band is due to the formation of fluorenone from monoalkyl fluorene (Chart 1) in the polymer backbone and effective energy transfer from polymer backbone to fluorenone, which is testified by the model systems of monoalkyl polyfluorene and fluorene/fluorenone copolymers.[3] However, the understanding of these interrelated properties is still debatable. The aggregate emission cannot explain that: (a) the low-energy emission still emerges in the presence of a bulky side group, which increases the molecular distance far from $\pi-\pi$ interaction distance; (b) PF showed spectral stability when annealed in a vacuum, and LPPP showed low-energy emission in dilute solution; and (c) the absence of a $\pi-\pi$ interaction in the single crystal structures of fluorene-based polymers and oligomers, which is the reason that fluorenone emission is proposed.[4] Yet the fluorenone emission also cannot explain the incompatibility

CHART 1: Molecular Structures of LPPP, PF, and LPFs and Defect Structures in PFs

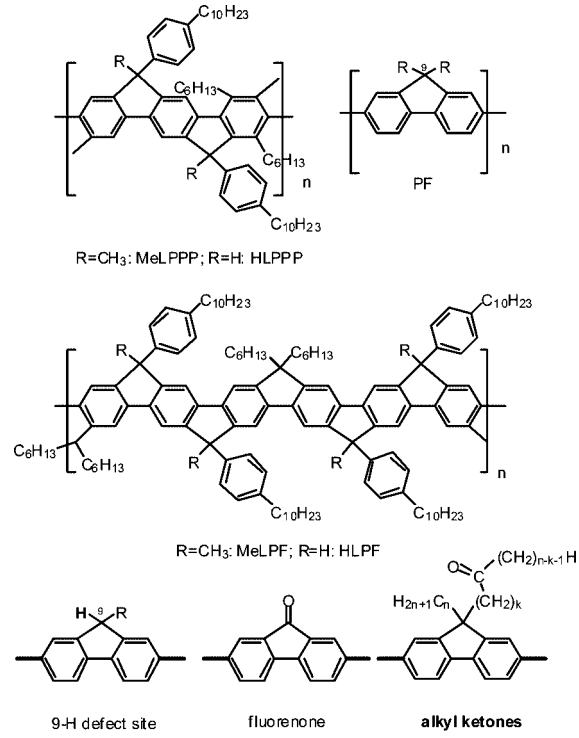

of the concentration of fluorenone and the intensity of low-energy emission in degraded kinetics of many different fluorene-based systems.[5] To explain it, a new hypothesis is claimed by Sims et al. that fluorenone formation is a necessary but not sufficient condition of the appearance of the low-energy band, and the additional interchain interactions are required for the appearance of the low-energy band (e.g., fluorenone excimers).[5a,b] Yet at the same time, the observations, which support the on-

* Corresponding author. Fax: (+86) 431-85168480. E-mail: ygma@jlu.edu.cn.

10.1021/jp8090733 CCC: $40.75
Published on Web 03/17/2009

chain fluorenone defect emission from single polyfluorene molecules in the absence of the intermolecular interactions, are reported.[5c,d] In one word, it is difficult to explain some phenomena in the degradation of PFs by either fluorenone defect or aggregation/excimer emission. In our earlier works, the third factor was proposed to explain the complex spectroscopic behavior of degraded PFs; that is, alkyl ketone (Chart 1) formed in degradation besides fluorenone can play a role as a nonemissive quencher for both emissions from PF and fluorenone.[6] However, the real chromophore group is still the key point to solve the stability of PFs, for different chromophore groups (aggregate or fluorenone) require different structural design to strain low-energy emission and increase stability. Thus, we try to determine the real chromophore group in fluorene-based compounds.

To our knowledge, all possible structures of the real chromophore group for the low-energy emission include fluorene−fluorene aggregate/excimer, fluorene−fluorenone aggregate/exciplex, fluorenone−fluorenone aggregate/excimer, and fluorenone itself, which would be mainly divided into intermolecular structure (fluorene and/or fluorenone-based aggregate in ground and excited state) and intramolecular structure (fluorenone). To divide these entities, a defectless polymer is required first for ensuring the fluorene−fluorene aggregate/excimer. Normally a very low concentration of defects, which is difficult to characterize by the general analysis methods of IR and NMR, can show strong green emission, misleading the investigation. Second, we need to find a suitable method to divide aggregate from fluorenone, which show many similar spectroscopic behaviors such as low-energy emission and complex behavior in excited states. In PFs, a more special phenomenon is that no matter the emission from fluorenone or aggregate, strong green emission must be observed in solid state for the effective energy transfer is necessary. Previous researches have testified the absence of $\pi-\pi$ interaction in the single crystal structures of fluorene-based polymers and oligomers.[4e] Assuming aggregate emission, the probability of interchain interaction in fluorene-based compounds would be very small, which only depends on the aggregate of end-groups, defect, and so on. Thus, strong green emission must be observed under effective energy transfer. For the low oscillator strength and quantum efficiencies of fluorenone-containing materials,[3h] the strong green emission of PFs is also regarded as an efficient energy transfer from dialkyl fluorene segments to the fluorenone defects.[3] Thus, nice blue emission in dilute solution but green emission in solid film is the typical behavior of PF, and it is difficult to determine the real role of condensed matter. Here, we plan to divide them by molecular-distance-dependent emission based on different effective interaction distances between energy transfer only (Föster radius 5−10 nm) and intermolecular interaction (excimer/exciplex distance less than 0.4 nm).[7] At last, a model compound with stable morphology in solid state is needed, for morphology of PFs is too complex, which is from the rotatable carbon−carbon single bond, side chain crystallization, and so on.[1a]

Previously, we have reported the defectless ladder-type copolymers LPFs (Chart 1) that have the fluorene units in the backbone.[6a] They have typical bridged bonds both in PF and in LPPP and so the similar low-energy emission. Especially the rigid backbone induces specific morphology, spectroscopy, and stable thermal properties, which would be a good model to reveal the origin of low-energy emission. In this article, we report the morphology and optical properties of these two fluorene-based ladder-type PPPs, MeLPF and HLPF, and try to explore the origin of low-energy emission of LPFs.

Experimental Section

Instrumentation and Sample Preparation. UV−vis and fluorescence spectra were obtained on a Shimadzu UV-3100 spectrophotometer and a Shimadzu RF-5301PC spectrophotometer, respectively. The cast polymer film was detected with a Rigaku X-ray diffractometer (XRD) (D/max r A, using Cu Kα radiation of wavelength 1.542 Å). Atom force microscope (AFM) images were recorded under ambient conditions using a Digital Instrument Multimode Nanoscope IIIa operating in the tapping mode. Si cantilever tips (TESP) with a resonance frequency of approximately 300 kHz and a spring constant of about 40 N m^{-1} were used. The scan rate varied from 0.5 to 1.5 Hz. LPF was dissolved in toluene or chloroform. Solutions were stored in sealed vials in an inert atmosphere in the dark in a refrigerator at about 280 K. To get good dispersion of HLPF in polycarbonate (PC), the solutions were heat-treated at 80 °C before spin-coating. Samples for XRD and AFM were cast onto silicon substrates and spin-coated on quartz substrate, respectively.

Materials. MeLPF and HLPF were synthesized by bridging fluorene-based poly(*para*-phenylene) precursors as described before.[6a] The number-average molecular weights (M_n) of MeLPF and HLPF are 22 000 and 16 000 (determined by gel permeation chromatography (GPC)), corresponding to a degree of polymerization of ∼70 and 50 *para*-phenylene subunits in the backbone, and the polydispersity index was measured to be 1.92 and 1.65, respectively. PC resins were purchased from J&K Chemical, Ltd., with the weight-average molecular weights (M_w) of 45 000.

Results and Discussion

We present experimental results obtained for two fluorene-based ladder-type polymers, MeLPF and HLPF. The difference between the two molecules resides in one of the side chains at the bridge; HLPF has a hydrogen atom, while in MeLPF the hydrogen is replaced by a methyl group (Chart 1). MeLPF and HLPF exhibit good thermal stability measured by thermogravimetric analysis (TGA) under a nitrogen atmosphere. The polymers have onset degradation temperatures (T_d) above 358.3 and 400.9 °C, respectively, which is related to thermal stability of different 9-substitution. No weight loss is observed at lower temperatures. The phase transitions of the polymers were determined by differential scanning calorimetry (DSC) in a nitrogen atmosphere at a heating rate of 5 K/min, but we observed neither a glass transition process (T_g) nor any other thermal process (such as liquid-crystal phase) from 20 to 300 °C for MeLPF and HLPF.[6a] As discussed above, stable morphology is one of the necessary conditions for exploring the origin of low-energy emission.

Morphological Behavior and Optical Properties of LPFs. The polymer structures in solid state are studied by XRD and AFM. Figure 1 shows the XRD patterns of the MeLPF and HLPF. The diffraction pattern of MeLPF shows a sharp peak at 6.6° and a broad peak at 19.0°, which correspond to *d* spacings at 13.5 and 4.8 Å, respectively. This type of pattern of MeLPF is similar to those observed in PFs or PIFs (polyindenofluorenes).[8] The origin of low-angle diffraction peak at 13.5 Å is assigned to the average distance between polymeric backbones.[8] The periodicity of 4.8 Å would reflect the spacing between adjacent side chains along the polymer backbone and corresponds to side-chain segregation.[8] For the long side chain of LPPP unit ($C_{10}H_{21}-$), this repeat distance (4.8 Å) is larger than PF (PIF) or aryl-substituted PF (PIF), which is about 4.2−4.3 Å (normally $C_6H_{13}-$ or $C_8H_{17}-$).[8] Despite only replacing methyl by hydrogen, the diffraction pattern of HLPF

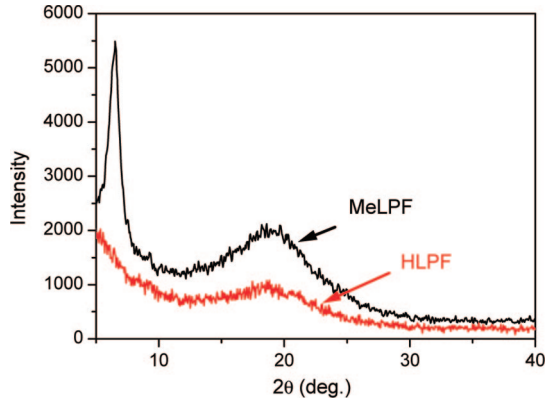

Figure 1. X-ray diffractogram of MeLPF and HLPF films.

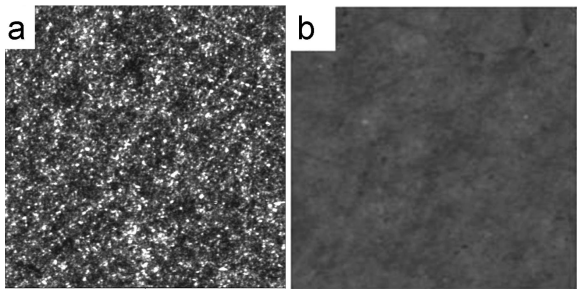

Figure 2. AFM high images of spin-coating film on quartz plate substrates from 1 mg/mL toluene solution 5 × 5 μm^2 with a vertical gray scale of 15 nm: (a) MeLPF, (b) HLPF.

is quite different from that in MeLPF, which just shows a side-chain segregation peak at 19.0° with a repeat distance of 4.8 Å. The AFM high images of the spin-coating films of the polymers also describe the different film morphology between MeLPF and HLPF. Figure 2 shows AFM high images of LPFs spin-coating films in the same condition. MeLPF film shows a rather rough morphology with a root-mean-square (RMS) roughness of 1.5 nm. In contrast, HLPF film clearly has a fairly smooth surface morphology with a RMS roughness of 0.3 nm.

Theoretically, the LPPP chain is a two-dimensional planar structure, which tends to strongly pack in the solid state. However, the morphology of MeLPF is just somehow similar to PFs and PIFs, and that of HLPF shows less order, as were the results from XRD and AFM measurements. The origin of less order is clearly not from the incomplete ring-closing reaction, for PFs and PIFs also pack in solid states. HLPPP (Chart 1) is the most typical one, which is expected to form more aggregate for its small substitution at the beginning, but then testified a simple −H (HLPPP) in the presence of other much more bulky substituents would not play such a role.[9] Small-angle X-ray and neutron scattering suggest HLPPP exhibits a three-dimensional spatial structure with chains degree of about 20−30°, but not the expected plane two-dimensional structure.[10] The less ordered morphology of LPFs, especially HLPF here, also seems to relate to the real topological structure of the totally rigid inflexible structure in LPPP backbone, which would depend on the structure of the side chain.

Figure 3 shows absorption and PL spectra of MeLPF and HLPF in (a) dilute solution and (b) film. LPFs display a steep absorption edge and well-resolved vibrational energy band, which indicates a rigid π-system, and the PL spectra are mirror-plane symmetrical with the absorption spectra with a very small Stokes shift and large overlap of 0−0 band between UV and PL spectra, as described before.[6a] The two most remarkable results from these pictures are: (a) the corresponding peak position of MeLPF is 7 nm red-shifted as compared to that of HLPF, which indicates the different effective conjugation length in these polymers.[11] A similar report is from the comparison between MeLPPP and HLPPP,[3d] which may further testify the topological structure of the totally rigid inflexible LPPP backbone. (b) Although PL spectra in the solid state of MeLPF are almost identical to that in dilute solution, the hydrogen-substituted one (HLPF) shows clear low-energy emission in the solid state in agreement with the literature,[1b] which first regarded it as an aggregate and then from fluorenone emission.[3d,4b] Correlating the results from morphology and optical properties, low-energy emission is not observed in the more ordered MeLPF, but the HLPF. The intensity of low-energy emission is not corresponding to the degree of order in LPFs, and there is no direct relationship between morphology and low-energy emission.

Optical Properties of Pristine and Degraded LPF. As described above, there is a small Stokes shift and large overlap of 0−0 band between UV and PL spectra in LPFs, which would induce an effective reabsorption by themselves and strong concentration and thickness dependence of emission properties in solution and solid state. Figure 4 shows the emission spectra of the MeLPF in toluene solutions with different concentration, which is normalized by the 0−1 band. With increasing concentration, the relative intensities of the 0−0 band decrease, and a small spectral red-shift emerges of the 0−0 band, which can be understood by higher absorption in low wavelength. These are typical phenomena of reabsorption, which indicate the effective energy immigration between different polymer chains and imply an effective energy transfer to low-energy sites if some defect sites or aggregation/excimer exist in this system. The remarkable results in MeLPF are that low-energy emissions coincide with each other in different concentrations, which testify the absence of defect or aggregation/excimer in pristine MeLPF.

Heat treatment of films is used to introduce defect sites into polymer chain. LPFs cast films are heated at 200 °C in air for 2 h to obtain the degraded films, which show clear low-energy emission band at 520 nm. The degraded LPFs can be resoluted by toluene for investigation of optical properties, which help to understand the origin of low-energy emission. Figure 5a shows the emission spectra of pristine and degraded MeLPF in diluted toluene solutions (50 μg/mL) at room temperature. Normalized by the 0−1 band, the 0−0 emission is quenched more in degraded MeLPF, and their low-energy emission is a little higher than the pristine one. These phenomena are clearer at low temperature as shown in Figure 5b. Pristine MeLPF displays two additional vibrational energy bands at 77 K as compared to at room temperature, for the restrain of vibrational quenching at low temperature. Vibrational structure is strongly suppressed in degraded MeLPF, and the relative intensity of low-energy emission is higher, which indicate the low-energy emissive species produced by heat treatment in air. These phenomena testify that low-energy emission can be observed in dilute solution where the intermolecular distance is far. However, in agreement with the literature and the data above, the intensity of low-energy emission in solution is not as remarkable as that in condensed matters.

Figure 6a shows the emission spectra of pristine MeLPF cast film with different thickness of ~5, 50, and 300 nm, which is cast from solutions with different concentrations. Thickness dependence emission presents behavior similar to that of concentration-dependent ones as shown in Figure 3, that relative intensities of the 0−0 band decrease with increasing film

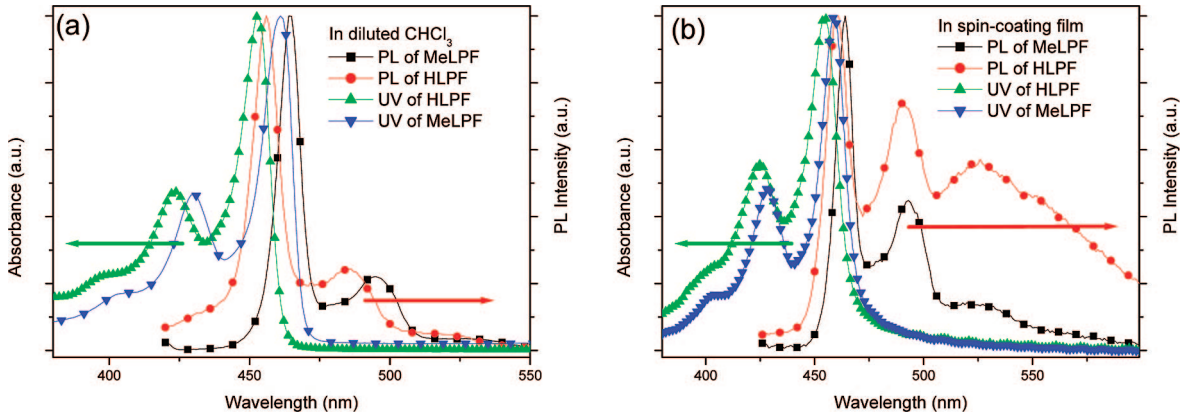

Figure 3. Absorption and PL spectra of MeLPF and HLPF (a) in dilute solution and (b) as spin-coating films. The spectra are normalized by the 0−0 band, and the PL spectrum is excited at 400 nm.

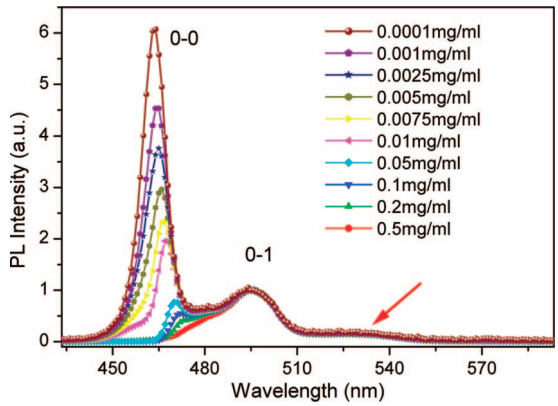

Figure 4. The emission spectra of the MeLPF in toluene solutions with different concentrations. The spectra are normalized by the 0−1 band, and PL spectra are excited at 400 nm.

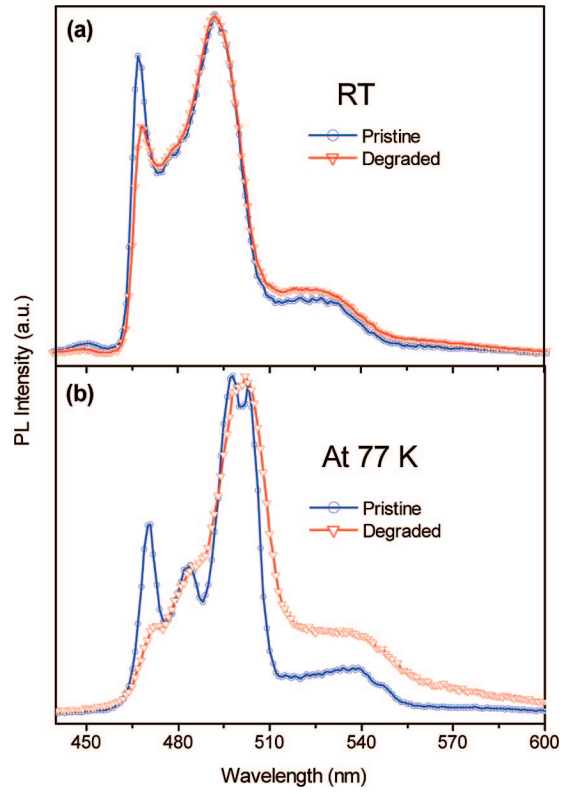

Figure 5. The emission spectra of pristine and degraded MeLPF in diluted toluene solutions (50 μg/mL) (a) at room temperature and (b) at 77 K. The spectra are normalized by the 0−1 band, and PL spectra are excited at 400 nm.

thickness. For the small distance between adjacent polymer chains in the solid state, we suppose Förster energy transfer, which is also strongly dependent on overlap between absorption and emission spectra, is the main route of energy transfer, and is much more effective than reabsorption. The low-energy emissions still are very small and coincide with each other in different thickness. Figure 6b shows the emission spectra of degraded MeLPF cast film, which bear the same condition as in Figure 6a. The low-energy emission is much higher than that in pristine MeLPF and increases step by step with the increasing film thickness, which comes from more effective energy transfer to emissive degraded products in thicker film. All of the results support that the low-energy emission is strongly related to degraded products but no aggregate/excimer in pristine MeLPF, similar to previous reports. By comparing the optical properties of pristine and degraded Me-LPF, low-energy emission in fluorene-based compounds and polymers is testified relating to oxidized products, which would be fluorenone or fluorenone-based aggregate. HLPF shows optical behavior similar to that of degraded MeLPF. Defectless MeLPF is chosen in this section to explore the basic role of degradation.

Evolution of Low-Energy Emission in Degraded LPF in Inert Polymer Matrix. Here, we try to determine the real chromophore group, with fluorenone-based aggregate and fluorenone as candidates. As described above, we plan to distinguish them by molecular-distance-dependent emission based on different effective interaction distances between energy transfer only (Föster radius 5−10 nm) and intermolecular interaction (excimer/exciplex distance less than 0.4 nm). Degraded LPF is doped into inert polymer (polycarbonate PC) to control molecular distance in series. HLPF is chosen for its amorphous phase behavior. It is of importance to note the solubility of HLPF in PC. Here, we try to describe it from two points of view. First, the morphology of the PC/d-HLPF spin-coating film is observed to detect the phase behavior of blends ($\leq$10%), which are very smooth without any type of phase separation and testify HLPF is well dispersed in PC matrix. Second, we try to use the Hildebrand solubility parameters to test the solubility of HLPF in PC matrix on molecular level. Although there is no report about the absolute Hildebrand solubility parameters of LPPP-type polymer, it can be determined by the solubility in organic solvent (chlorobenzene δ = 9.5) with the same Hildebrand solubility parameters of PC (δ = 9.5). The good solubility of HLPF in chlorobenzene strongly supports the well-dispersed HLPF in PC matrix.

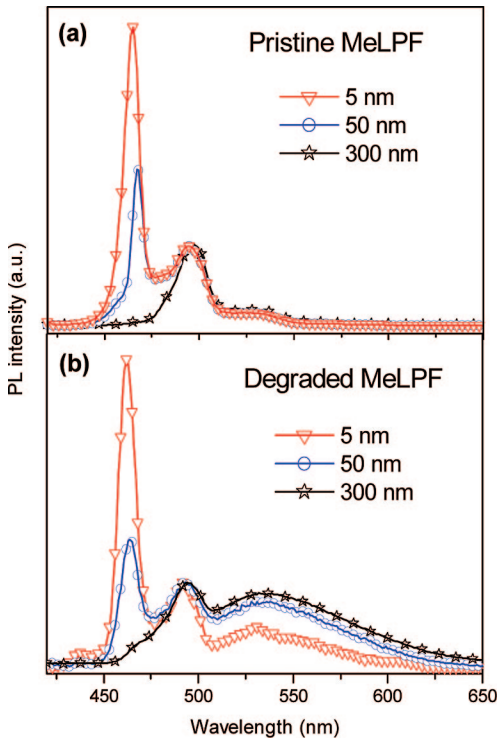

Figure 6. PL spectra of pristine (a) and degraded (b) MeLPF cast film with different thickness. The spectra are normalized by the 0−1 band, and PL spectra are excited at 400 nm.

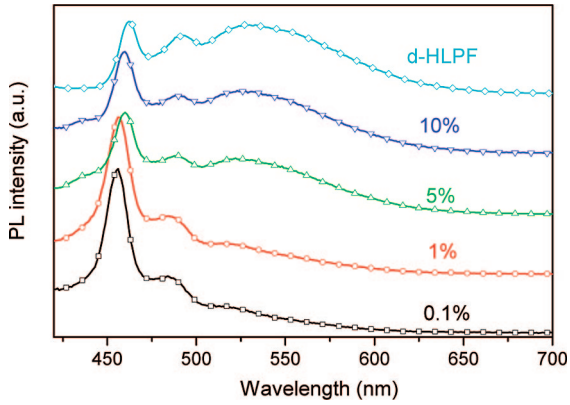

Figure 7. PL spectra for different concentrations of degraded HLPF (d-HLPF) in PC matrix specified in the legend. The emission of the d-HLPF spin-coated film is also given as a comparison (normalized by the 0−1 emission band and excited at 360 nm).

Figure 7 shows emission spectra for different concentrations of degraded HLPF (d-HLPF) in PC matrix. For the ratios of d-HLPF of 0.1% and 1%, the low-energy emissions are very small. Clear low-energy emission is observed when the ratio of d-HLPF is larger than 5%, and after 10% the low-energy emission is as high as that of d-HLPF spin-coated film. To extract the exact nature from these data sets, the relative intensity of low-energy emission is calculated for all blend systems and plotted versus the concentration of d-HLPF. As depicted in Figure 8, for low d-HLPF concentration (<10%), the relative intensity of low-energy emission is weak. For higher fluorenone concentration (>10%), the low-energy emission is strong and increases smoothly.

Assuming d-HLPF molecule is a mass point in the center of a cube and a continuous distribution of the two components of the polymer blend on molecular level, the intermolecular distance between adjacent d-HLPF molecules is estimated by

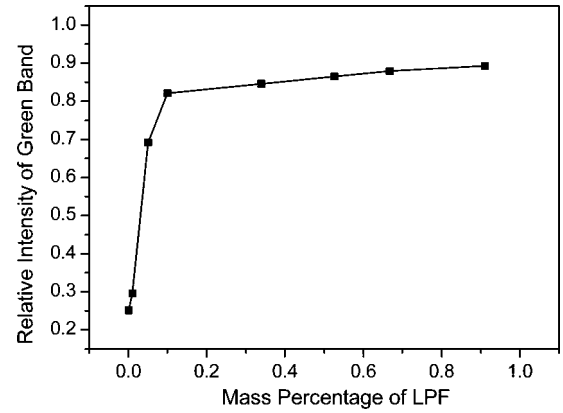

Figure 8. Relative intensity of low-energy emission as a function of d-HLPF concentration (normalized by the 0−1 emission band) .

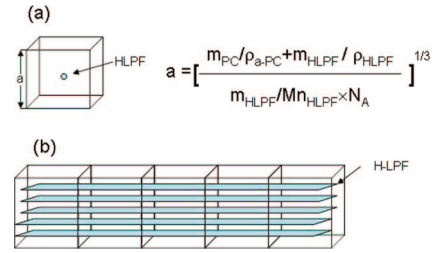

Figure 9. (a) Estimate of intermolecular distance assuming HLPF molecule is a mass point in the center of a cube, and (b) a five HLPF chain standing face to face in five continuous cubes.

the formula shown in Figure 9a. Here, a is the length of cube side and intermolecular distance, m is mass, N_A is Avogadro's number, and ρ is density (density of amorphous PC is 1.20 g/cm^3, assuming density of HLPF is 1.0 g/cm^3). The intermolecular distance is about 6 nm at a ratio of PC/d-HLPF of 10%, which is enough for an effective Förster energy transfer, but too far to form an intermolecular interaction such as excimer. Considering the linear structure of HLPF (50 *para*-phenylene, about 30 nm length), the most possible structure to form intermolecular interaction is five HLPF chains standing face to face in five continuous cubes (Figure 9b). In this case, the average distance between adjacent HLPF chains is 1.2 nm, which is also far from effective intermolecular interaction. Thus, the low-energy emission must be from effective Förster energy transfer to emissive point. Considering the molecular aggregate (dimer or excimer), this distance would be larger and the low-energy emission should tend to increase continuously with the increasing ratio of HLPF while decreasing molecular distance. Thus, we can ensure this crucial point is not from the aggregate of HLPF in PC matrix, and the real chromophore group is finally determined as fluorenone.

Conclusion

In conclusion, we report the morphology and optical properties of two fluorene-based ladder-type PPPs, MeLPF and HLPF. Different types of experiments are designed to distinguish the real chromophore group of low-energy emission of LPFs from aggregate to defect. The presented experimental evidence rules out excimers and aggregate as the source of the low-energy emission in fluorene-based polymers including fluorenone-based aggregate and suggests fluorenone as the real chromophore group.

Acknowledgment. We thank Professor Soo Young Park for his helpful suggestions, and we are grateful for financial support

from National Science Foundation of China (grant numbers 20573040, 20834006), the Ministry of Science and Technology of China (grant number 2002CB6134003), the 111 project (B06009), and PCSIRT.

References and Notes

(1) (a) Scherf, U.; List, E. J. W. *Adv. Mater.* **2002**, *14*, 477. (b) Scherf, U. *J. Mater. Chem.* **1999**, *9*, 1853.

(2) (a) Kreyenschmidt, M.; Klaerner, G.; Fuhrer, T.; Ashenhurst, J.; Karg, S.; Chen, W. D.; Lee, V. Y.; Scott, J. C.; Miller, R. D. *Macromolecules* **1998**, *31*, 1099. (b) Lee, J. I.; Klärner, G.; Miller, R. D. *Chem. Mater.* **1999**, *11*, 1083. (c) Lemmer, U.; Heun, S.; Mahrt, R. F.; Scherf, U.; Hopmeier, M.; Siegner, U.; Göbel, E. O.; Müllen, K.; Bässler, H. *Chem. Phys. Lett.* **1995**, *240*, 373. (d) Cimrová, V.; Scherf, U.; Neher, D. *Appl. Phys. Lett.* **1996**, *69*, 608. (e) Bliznyuk, V. N.; Carter, S. A.; Scott, J. C.; Klärner, G.; Miller, R. D.; Miller, D. C. *Macromolecules* **1999**, *32*, 361.

(3) (a) List, E. J. W.; Guentner, R.; Scandiucci de Freitas, P.; Scherf, U. *Adv. Mater.* **2002**, *14*, 374. (b) Romaner, L.; Pogantsch, A.; Scandiucci de Freitas, P.; Scherf, U.; Gaal, M.; Zojer, E.; List, E. J. W. *Adv. Funct. Mater.* **2003**, *13*, 597. (c) Gong, X.; Iyer, P. K.; Moses, D.; Bazan, G. C.; Heeger, A. J.; Xiao, S. S. *Adv. Funct. Mater.* **2003**, *13*, 325. (d) Romaner, L.; Heimel, G.; Wiesenhofer, H.; Scandiucci de Freitas, P.; Scherf, U.; Brédas, J.-L.; Zojer, E.; List, E. J. W. *Chem. Mater.* **2004**, *16*, 4667. (e) Yang, X. H.; Jaiser, F. J.; Neher, D.; Lawson, P. V.; Brédas, J.-L.; Zojer, E.; Güntner, R.; Scandiucci de Freitas, P.; Forster, M.; Scherf, U. *Adv. Funct. Mater.* **2004**, *14*, 1097. (f) Zhao, W.; Cao, T.; White, J. M. *Adv. Funct. Mater.* **2004**, *14*, 783. (g) Chi, C. Y.; Im, C.; Enkelmann, V.; Ziegler, A.; Lieser, G.; Wegner, G. *Chem.-Eur. J.* **2005**, *11*, 6833. (h) Zojer, E.; Pogantsch, A.; Hennebicq, E.; Beljonne, D.; Brédas, J.-L.; List, E. J. W. *J. Chem. Phys.* **2002**, *117*, 6794. (i) Li, J.; Li, M.; Bo, Z. S. *Chem.-Eur. J.* **2005**, *11*, 6930.

(4) (a) Gaal, M.; List, E. J. W.; Scherf, U. *Macromolecules* **2003**, *36*, 4236. (b) Lupton, J. M. *Chem. Phys. Lett.* **2002**, *365*, 366. (c) Chen, S. H.; Chou, H. L.; Su, A. C.; Chen, S. A. *Macromolecules* **2004**, *37*, 6833. (d) Chi, C. Y.; Lieser, G.; Enkelmann, V.; Wegner, G. *Macromol. Chem. Phys.* **2005**, *206*, 1597. (e) Chen, S. H.; Su, A. C.; Su, C. H.; Chen, S. A. *Macromolecules* **2005**, *38*, 379.

(5) (a) Sim, M.; Bradley, D. D. C.; Ariu, M.; Koeberg, M.; Asimakis, A.; Grell, M.; Lidzey, D. G. *Adv. Funct. Mater.* **2004**, *14*, 765. (b) Chochos, C. L.; Kallitsis, J. K.; Gregoriou, V. G. *J. Phys. Chem. B* **2005**, *109*, 8755. (c) Becker, K.; Lupton, J. M.; Feldmann, J.; Nehls, B. S.; Galbrecht, F.; Gao, D.; Scherf, U. *Adv. Funct. Mater.* **2006**, *16*, 364. (d) Marcon, V.; van der Vegt, N.; Wegner, G.; Raos, G. *J. Phys. Chem. B* **2006**, *110*, 5253.

(6) (a) Qiu, S.; Lu, P.; Liu, X.; Shen, F. Z.; Liu, L. L.; Ma, Y. G.; Shen, J. C. *Macromolecules* **2003**, *36*, 9823. (b) Liu, L. L.; Qiu, S.; Wang, B.; Zhang, W.; Lu, P.; Xie, Z. Q.; Hanif, M.; Ma, Y. G.; Shen, J. C. *J. Phys. Chem. B* **2005**, *109*, 23366. (c) Liu, L. L.; Tang, S.; Liu, M. R.; Xie, Z. Q.; Zhang, W.; Lu, P.; Hanif, M.; Ma, Y. G. *J. Phys. Chem. B* **2006**, *110*, 13734. (d) Liu, L. L.; Lu, P.; Xie, Z. Q.; Wang, H. P.; Tang, S.; Wang, Z. M.; Zhang, W.; Ma, Y. G. *J. Phys. Chem. B* **2007**, *111*, 10639. (e) Liu, L. L.; Yang, B.; Zhang, H. Y.; Tang, S.; Xie, Z. Q.; Wang, H.; Wang, Z. M.; Lu, P.; Ma, Y. G. *J. Phys. Chem. C* **2008**, *112*, 10273.

(7) (a) Turro, N. J. *Modern Molecular Photochemistry Chinese Press*; Science Press: China, 1987. (b) List, E. J. W.; Leising, G. *Synth. Met.* **2004**, *141*, 211.

(8) Keivanidis, P. E.; Jacob, J.; Oldridge, L.; Sonar, P.; Carbonnier, B.; Baluschev, S.; Grimsdale, A. C.; Müllen, K.; Wegner, G. *ChemPhysChem* **2005**, *6*, 1650.

(9) Lemmer, U.; Heun, S.; Mahrt, R. F.; Scherf, U.; Hopmeier, M.; Siegner, U.; Göbel, E. O.; Müllen, K.; Bässler, H. *Chem. Phys. Lett.* **1995**, *240*, 373.

(10) Hickl, P.; Ballauff, M.; Scherf, U.; Mullen, K.; Lindner, P. *Macromolecules* **1997**, *30*, 273.

(11) Grimme, J.; Kreyenschmidt, M.; Uckert, F.; Mullen, K.; Scherf, U. *Adv. Mater.* **1995**, *7*, 292.

JP8090733